

DYNAMICS OF AN ELECTRON IN AN RF GAP*

Z. D. FARKAS AND P. B. WILSON

*Stanford Linear Accelerator Center**Stanford University, Stanford, California 94309***ABSTRACT**

The purpose of this calculation is to understand the limitation on the energy transfer efficiency of an electron beam to the RF field in the output cavity of a klystron or a lasertron. An output cavity with drift tubes is modeled in this calculation by a region of constant amplitude RF field with exponentially decreasing entrance and exit fringing fields. The exit velocity of an electron traversing such a gap is examined as a function of entrance phase for various values of the ratio of the peak RF cavity voltage to electron entrance voltage. Depending on this ratio, the dynamics of the electron motion can become quite complex. For a gap with fringe fields it is found that, even if the gap voltage and phase are optimized, the maximum energy that can be extracted from a short bunch is always significantly less than 100%. The case in which the electron is created with zero velocity in the gap, and subsequently leaves the gap having extracted energy from the RF field, is also treated.

1. INTRODUCTION

J. Welch has previously found,¹ using the MASK simulation code, that a short electron bunch cannot deliver more than about 80% of its energy to an RF gap of the type used in the SLAC lasertron experiment and in most klystrons. He further found that this limit on efficiency is present using even a crude one-dimensional model of the gap in which the bunch is replaced by a single electron interacting

(Submitted for Publications)

* Work supported by the Department of Energy, contract DE-AC03-76SF00515.

with the RF field. In the present note, this problem is pursued further. The electron motion is examined in some detail in terms of normalized gap parameters, both for relativistic and nonrelativistic examples. We first write down the difference equations for the electron motion and then apply them to the case of a plane-parallel gap with no fringing field. We next apply them to the case of a typical klystron output cavity with drift tubes, modeled by a region of constant amplitude RF field with exponentially decreasing entrance and exit fringe fields, as shown in Fig. 1. Also shown in Fig. 1 is the field, obtained using SUPERFISH, for the output cavity of the X100 high power X-band klystron now under development at SLAC.² The position and velocity of the electron as functions of time are obtained by integrating the equations of motion through the gap, starting from an entrance position in a region of negligible RF field. The subsequent motion of the electron depends strongly on the phase of the RF field (the entrance phase) at the time the electron leaves this entrance position. Of particular interest is the exit velocity of the electron, after it has left the gap either by transmission or reflection. The exit velocity (and energy) is examined as a function of entrance phase for different values of the ratio of the peak RF gap voltage to the electron entrance voltage.

2. EQUATIONS OF MOTION

2.1. List of Symbols

E_o = RF peak voltage

ω = RF (angular) frequency

g = gap length (length of uniform field region)

b = cutoff tube attenuation parameter

V_o = initial electron voltage

α = ratio of RF gap voltage to initial voltage, $\alpha = E_o g / V_o$

z = electron position along the gap

Z = normalized position, z/g

v = electron velocity

ν = electron velocity normalized to the entrance velocity, $\nu = v/v_o$

p = electron momentum

P = electron momentum normalized to the entrance momentum, $P = p/p_0$

W = ratio of electron exit energy to electron initial energy, $W = w/w_0$

$\delta\phi$ = phase (time) step, $\delta\phi = \omega\Delta t$

ϕ_g = gap transit angle, $\phi_g = \omega g/v_0$

ϕ_0 = initial phase

ϵ = relative phase (time) advance, $\epsilon \equiv \delta\phi/\phi_g$, per phase step

n = phase step index number

ϕ_n = phase at step n , $\phi_n = \phi_0 + n\delta\phi$

ϕ_t = total cumulative phase when the electron exits the gap

D_t = time that electrons spend in the gap in units of RF period

γ = relativistic energy parameter, $\gamma = 1 + eV/m_0c^2$

$\beta = v/c$

c = velocity of light

2.2. Nonrelativistic Case

The equations of motion in the nonrelativistic case are

$$v_{n+1} = v_n + \frac{eE}{m} \Delta t$$

$$z_{n+1} = z_n + v_{n+1} \Delta t$$

In normalized form, the equations of motion become

$$\phi_{n+1} = \phi_n + \delta\phi$$

$$\nu_{n+1} = \nu_n + (\alpha\epsilon/2)F_z \cos\phi_n$$

$$Z_{n+1} = Z_n + \epsilon\nu_{n+1} \quad ,$$

where

$$F_z = 1 \quad |Z_n| < 0.5$$

$$F_z = \exp[-b(|Z_n| - 0.5)] \quad |Z_n| > 0.5$$

Here $Z = z/g$ is the normalized position, g is the length of the region of uniform gap field, E_0 , and $\nu = v/v_0$ is the normalized velocity where v_0 is the entrance velocity. The normalized gap voltage is $\alpha \equiv E_0g/V_0$, where V_0 is the electron entrance voltage. The time step parameter is $\delta\phi = \omega\delta t = e\phi_g$, where $\phi_g = \omega g/v_0$ is the gap transit angle. The fringe fields are assumed to decay with distance in the drift tube as $E \sim E_0 \exp[-b/g (|z| - g/2)]$. The normalizing velocity v_0 is obtained from

$$\frac{1}{2} m v_0^2 = \frac{e E_0 g}{\alpha} \quad ; \quad v_0 = \sqrt{\frac{2e E_0 g}{\alpha m}}$$

2.3. Relativistic Case

The equations of motion for the relativistic case are:

$$p_{n+1} = p_n + eE\Delta t$$

$$z_{n+1} = z_n + v_{n+1}\Delta t \quad ,$$

where $p_n = \beta_n \gamma_n m_0 c$. The normalizing momentum, velocity and energy are:

$$p_0 = \gamma_0 \beta_0 m_0 c = m_0 c \sqrt{\gamma_0^2 - 1} \quad , \quad \beta_0 = \frac{\sqrt{\gamma_0^2 - 1}}{\gamma_0} \quad , \quad w_0 = (\gamma_0 - 1) m_0 c^2 \quad ,$$

$$\gamma_0 = 1 + \frac{Eg}{\alpha V_e} \quad , \quad V_0 = (\gamma_0 - 1) V_e \quad ,$$

where $V_e = m_0 c^2/e = 0.511$ mV. In normalized form, the equations of motion in the relativistic case are

$$\phi_{n+1} = \phi_n + \delta\phi$$

$$P_{n+1} = P_n + \alpha \epsilon \left[\frac{\gamma_0}{\gamma_0 + 1} \right] F_z \cos \phi_n$$

$$Z_{n+1} = Z_n + \epsilon \nu_n \quad ,$$

where

$$P_n = \frac{p_n}{p_o} = \frac{\beta_n \gamma_n}{\beta_o \gamma_o} \quad , \quad \gamma_n = \sqrt{1 + P_n^2 (\gamma_o^2 - 1)} \quad , \quad \nu_n = \frac{\beta_n}{\beta_o} = \frac{P_n \gamma_o}{\gamma_n} \quad .$$

The normalized energy is

$$W_n = \frac{w}{w_o} = \frac{\gamma_n - 1}{\gamma_o - 1} \quad .$$

Note that the equation for momentum in the relativistic case reduces to the non-relativistic expression as $\gamma \rightarrow 1$, as it should, and the dynamics of the electron become independent of the entrance energy.

3. GAP WITHOUT FRINGE FIELDS; NONRELATIVISTIC CASE

In order to delineate the effects due specifically to the fringing field, we first consider the case of a cavity without drift tubes (*e.g.*, a gridded gap). This would also approximate the case for a hollow beam, or for the electrons at the outer edge of a round beam near the walls of the drift tube. Simple analytic expressions can be written in this case for the electron velocity and position as a function of time and entrance phase. The value of α just required to bring an electron to rest at the output edge of the gap is $\alpha = \phi_g / \sin \phi_{0c}$, at an entrance phase $\phi_{0c} = \pi - \phi_g$ where $\phi_g < \pi$.

The normalized exit velocity as a function of entrance phase for the case $\phi_g = \pi/2$ is shown in Fig. 2 for a gap without fringe fields. Note that for $\alpha = \pi/2$ one electron is indeed just brought to rest at the output of the gap at $\phi_0 = 90^\circ$, but that the slope of the curve is infinite, and hence the efficiency would decrease rapidly with increasing phase width of the bunch. At higher α the plots become more complex. Figures 3 and 4 show detailed phase space (velocity vs. distance) plots for a range of entrance phases. The first singularity near $\phi_0 = 68^\circ$ on the curve for $\alpha = 2.6$ in Fig. 2 occurs at the point at which electrons are just turned back as they reach the exit of the gap, as seen in Fig. 4. For slightly higher values of ϕ_{0c} the particle makes a loop inside the gap but still exits in the positive z direction. At still larger values of ϕ_0 the electrons exit in the negative z direction before they can complete the loop. This accounts for the region of reflected electrons in the entrance phase range 90° – 125° in Fig. 2.

Figure 5 shows the energy extraction efficiency as a function of central entrance phase for rectangular bunch current distributions with a phase width of 60° . In the case of an output cavity driven by the beam, the phase would adjust itself to transfer the maximum energy from the beam to the RF field. However, as seen from Fig. 5, any electrons in the broad antibunch region will extract a substantial amount of energy from the cavity field. A relatively few number of electrons in this region can severely degrade the efficiency.

Figure 6 shows the maximum efficiency, and the phase at maximum efficiency, as a function of α for bunches 20° and 60° in width. Note that the efficiency reaches a maximum near $\alpha \approx 1.5$, then decreases at higher α . At very large α the efficiency can increase again for short bunches. However, most of the electrons in the bunch are reflected rather than transmitted under this condition, certainly an undesirable situation for a klystron.

4. GAP WITHOUT FRINGE FIELDS; RELATIVISTIC CASE

An example was calculated using the relativistic equations of motion for the case $\phi_g = \pi/2$, $b = 2.5$, $V_0 = 1.0$ MV ($\gamma_0 = 3.0$). These values correspond approximately to the parameters for the output cavity of the SLAC/LLNL SL4 relativistic klystron experiment.⁴ A set of plots, similar to those shown in Figs. 2 to 6 for the nonrelativistic case, are shown in Figs. 7 to 11. Note that the maximum energy extraction efficiency is significantly lower for the same values of b , ϕ_g , and bunch length than for the nonrelativistic case.

5. GAP WITH FRINGE FIELDS

We next look at the modification in the previous results produced by the addition of fringing fields with an exponential decay parameter $b = 2.5$ (see Fig. 1). Figure 12 shows distance vs. accumulated phase (time) for $\alpha = 3.0$. We see that electrons are either transmitted through or reflected from the gap region depending on the entrance phase. (The entrance phase is taken to be the phase of the RF field when

the electron is at $Z = -2$.) A small change in entrance phase (from $\phi_0 = -26.4^\circ$ to -26.0°) leads to a change from transmission to reflection. The exit velocity in both cases is comparable to the entrance velocity (the velocity is proportional to the slope of the curve.)

Figure 13(a) shows plots of normalized velocity vs. normalized distance along the gap axis (phase space plot) for the case when the electron slows down or even reverses its velocity in the gap, but exits with about the same velocity as the entrance velocity. Figure 13(b) illustrates cases in which the electrons are reflected, that is, they exit in the $-Z$ direction. Figure 13(c) illustrates a more interesting behavior: the electron exits with a minimum velocity of about 0.4, corresponding to an efficiency of 86%. Note that the velocity is nearly zero for $\alpha = 3$ at $Z \approx 1$. However, because of the fringe field, it is not possible for the electron to exit with this low a velocity. Figure 13(d) illustrates a case ($\alpha = 3$ and $\phi_o = -190$) for which the electron is accelerated during most of the time it is in the gap, exiting with more than double its initial velocity (about five times the initial energy).

Figure 14 shows the normalized exit velocity as a function of entrance phase as α increases from 0.2 to 2.6. Note that the dip at about -50° corresponds to the singularity near 70° in the case of the gap with no fringe field (see Fig. 2), but it is rounded and does not extend to $\nu = 0$. Note also that the region of reflected electrons develops very rapidly over a small range of $\alpha = 2.5$ to 2.6.

Figure 15 shows the exit velocity for the case $\alpha = 3$. The region near the critical phase between transmission and reflection is magnified in the lower curve, where the exit velocity is plotted as a function of the log of the phase difference ϕ_d from the critical phase, $\phi_d = \phi_{0c} - \phi_0$. As the critical phase is approached, the exit velocity oscillates with an exponentially decreasing entrance phase period, but never falling below $\nu = 0.35$. The pattern shows self-similarity, repeating on a scale that decreases by about $10^{1.5}$ from one cycle to the next. A phase space plot of trajectories for the case $\alpha = 3$ is given in Fig. 16 for 10° intervals in entrance phase.

The efficiency as a function of central entrance phase is shown in Fig. 17 for a 60° bunch with uniform current distribution. Note that for large α the efficiency is positive

only over a fairly narrow phase range near $\phi_0 = 0^\circ$. Most electrons outside the bunch are strongly accelerated, with a consequent deleterious effect on efficiency. Figure 18 shows the maximum efficiency and central bunch phase at maximum efficiency as a function of α for 20° and 60° bunches. As in the case of the gap with no fringe fields, the efficiency can increase again at large α , but again the bunch electrons are mostly reflected rather than transmitted (the region between the "ears" in Fig. 14).

Plots of normalized exit momentum and efficiency vs. initial phase for the relativistic case with $b = 2.5$, $\phi_g = \pi/2$ and $\gamma_0 = 3.0$ are given in Figs. 19 and 20. The plot for maximum efficiency as a function of α is given in Fig. 21. The efficiency reaches a maximum of 72% at $\alpha = 1.5$ for the 20° bunch, and 53% at $\alpha = 0.6$ for the 60° bunch. This can be compared with Fig. 18 for the nonrelativistic case, where $\eta_{max} = 74\%$ at $\alpha = 1.5$ for the 20° bunch and $\eta_{max} = 63\%$ at $\alpha = 0.9$ for the 60° bunch.

6. MOTION OF ELECTRONS CREATED IN THE GAP

Electrons with zero velocity can appear at any RF phase at any point in a gap, either by ionization in the beam region or by photo-emission from the gap surface. After spending some time in the gap, these electrons leave the gap either in the positive or negative Z direction with some velocity greater than zero. The time spent in the gap and the exit velocity depend on the RF phase at the time of the particle's appearance; this is illustrated in Fig. 22 for the nonrelativistic case for electrons created at the center of a gap with $\alpha = 1$, $b = 2.5$, and $\phi_g = \pi/2$. The average normalized exit energy is 0.12 in this example, with equal probability of the electron leaving in the $+z$ or $-z$ direction. The electron motion in phase space is shown in Fig. 23.

For the relativistic case, plots of normalized exit energy as a function of initial phase are shown in Fig. 24 for RF gap voltages, $V_{rf} = V_0$, ranging from 0.01 to 1 MV. Still higher gap energies give results which are essentially the same as the $V_0 = 1$ MV case. Likewise, the $V_0 = 0.01$ MV is essentially at the nonrelativistic limit. Note that the average normalized exit energy at $V_{rf} = 1$ MV is about 0.6, about five times the

average normalized exit energy for the nonrelativistic case. The phase space plots for $\gamma_0 = 3.0$ are shown in Fig. 25.

By specifying a frequency and a gap length, the actual energy and velocity are readily calculated. In the nonrelativistic example, as in the previous examples, the transit angle for an electron with a velocity v_o is specified to be $\pi/2$. Thus $v_o = 2\omega g/\pi$. The normalization energy is then $w_o = mv_o^2/2$ and the gap voltage is $E_o g = \alpha w_o/e$. The actual energy and velocity at any point, including the exit, are then

$$w = W \times w_o \quad , \quad v = \nu \times v_o \quad .$$

Electrons appearing with zero velocity anywhere in the gap can only take energy from the RF field and hence represent RF loading.

7. CONCLUSION

The beam dynamics of an electron in an RF gap are relatively complex, even for the case of a gap with uniform field and no fringing fields. For such a gap it is possible to extract all of the energy from an electron which has just the right entrance phase and energy. However, the efficiency falls off rapidly with increasing phase width of the bunch. If the gap has an exponentially decaying fringe field, the dynamics become still more complex. In this case, it is not possible for an electron to lose all of its energy, even in principle. In a real klystron beam, the effect of the fringing field depends on radial position. The effect of the RF magnetic field on the motion of off-axis electrons must also be taken into account in a real gap. In addition, collective effects and energy spread in the incident beam can also affect the efficiency. The simple one-dimensional, single-particle dynamics discussed here, however, gives an indication of the limit on the efficiency that can be obtained.

Both the nonrelativistic case and the case where electrons can reach relativistic velocities have been considered. In the nonrelativistic regime, the exit to entrance energy ratio is independent of entrance kinetic energy, and depends only on the ratio of the RF gap voltage to the electron entrance voltage. In the relativistic regime,

the exit to entrance energy ratio (normalized energy) does depend on the electron entrance voltage. In the highly relativistic limit, the normalized exit energy is again independent of entrance energy.

The energy extracted from the RF field by electrons created in the gap by ionization or photo emission has also been considered. The exit energy of a zero velocity electron appearing at the center of the gap depends on the value of the RF gap voltage, and of course on the RF phase at the moment of its creation. It is found that the loading is much more severe for a gap where the electrons can reach relativistic energies (RF gap voltage exceeding 200 kV or so).

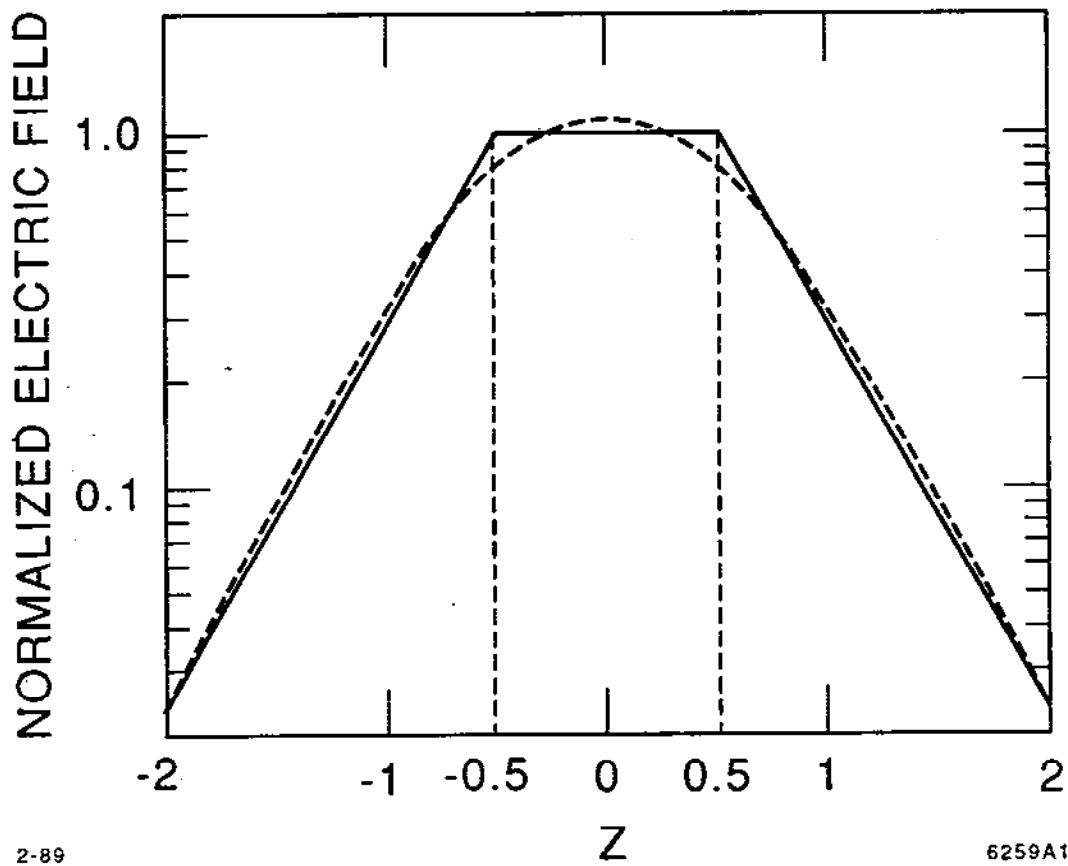
REFERENCES

1. J. J. Welch, 1986 Linear Accelerator Conference, SLAC-Report-303 (1986), pp. 25-86; also SLAC-PUB-3976 (1986).
2. T. Lee, private communication.
3. M. A. Allen *et al.*, SLAC-PUB-4733 (Sept. 1988); to be published in *Proceedings of the 1988 Linear Accelerator Conference*, Williamsburg, VA, October 3-7, 1988.

FIGURE CAPTIONS

- Fig. 1. Normalized electric field amplitude vs. normalized position. Dashed curve gives the field for the the SL4 klystron output cavity obtained with SUPERFISH.
- Fig. 2. Normalized exit velocity vs. entrance phase ($\phi_g = \pi/2$, no fringe fields, nonrelativistic).
- Fig. 3. Normalized velocity vs. distance ($\alpha = \pi/2$, no fringe fields, nonrelativistic).
- Fig. 4. Normalized velocity vs. distance ($\alpha = 2.6$, no fringe fields, nonrelativistic).
- Fig. 5. Efficiency vs. entrance phase for a 60° bunch, no fringe fields, nonrelativistic).
- Fig. 6. Maximum efficiency (solid) and entrance phase at maximum (dashed) efficiency vs. α , no fringe fields, nonrelativistic.
- Fig. 7. Normalized exit momentum vs. entrance phase ($\phi_g = \pi/2$, no fringe fields, relativistic, $V_o = 1$ MV).
- Fig. 8. Normalized momentum vs. distance ($\alpha = \pi/2$, no fringe fields, relativistic).
- Fig. 9. Normalized momentum vs. distance ($\alpha = 2.6$, no fringe fields, relativistic).
- Fig. 10. Efficiency vs. entrance phase for a 60° bunch, no fringe fields, relativistic.
- Fig. 11. Maximum efficiency (solid) and entrance phase at maximum efficiency (dotted) vs. α , no fringe fields, nonrelativistic.
- Fig. 12. Normalized distance vs. accumulated phase (time), for a gap with fringe fields, nonrelativistic $\alpha = 3.0$.
- Fig. 13. Normalized velocity vs. normalized distance for $\alpha = 2$ and $\alpha = 3$ and for various values of ϕ_0 , with fringe fields, nonrelativistic.
- Fig. 14. Normalized exit velocity vs. entrance phase, ($\phi_g = \pi/2$, $b = 2.5$), with fringe fields, nonrelativistic.
- Fig. 15. Normalized exit velocity as a function of entrance phase (top) and as a function of phase deviation from critical phase (bottom) for $\alpha = 3$.
- Fig. 16. Normalized velocity vs. normalized distance for $\alpha = 2$ at 10° intervals in entrance phase, gap with fringe fields, nonrelativistic.
- Fig. 17. Efficiency vs. entrance phase for a 60° bunch, gap with fringe fields, nonrelativistic.
- Fig. 18. Maximum efficiency (solid curves) and entrance phase at maximum efficiency vs. α , gap with fringe fields, nonrelativistic.

- Fig. 19. Normalized exit momentum vs. entrance phase for a gap with fringe fields, relativistic case, $V_0 = 1$ MV.
- Fig. 20. Efficiency vs. entrance phase for a 60° bunch, for gap with fringe fields, relativistic case with $V_0 = 1$ MV.
- Fig. 21. Maximum efficiency (solid) and entrance phase (dashed) at maximum efficiency vs. α , for a gap with fringe fields, relativistic case, $V_0 = 1$ MV.
- Fig. 22. Normalized exit velocity (solid) and dwell time (dashed) vs. initial phase for an electron created at $Z = 0$ with $\nu = 0$ ($\phi_g = \pi/2$, $b = 2.5$, $\alpha = 1$), gap with fringe fields, nonrelativistic case.
- Fig. 23. Phase space diagram for electrons originating with zero velocity at the gap midpoint for 10° intervals in initial phase, for a gap with fringe fields, nonrelativistic case.
- Fig. 24. Normalized exit energy vs. initial phase for electrons originating with zero velocity at the midpoint of a gap with fringe fields ($\phi_g = \pi/2$, $b = 2.5$, $\alpha = 1$), for several values of gap voltage.
- Fig. 25. Phase space diagram for electrons originating with zero velocity at the midpoint of a gap with fringe fields for 20° interval in entrance phase $V_{rf} = 1$ MV.



2-89

6259A1

Fig. 1

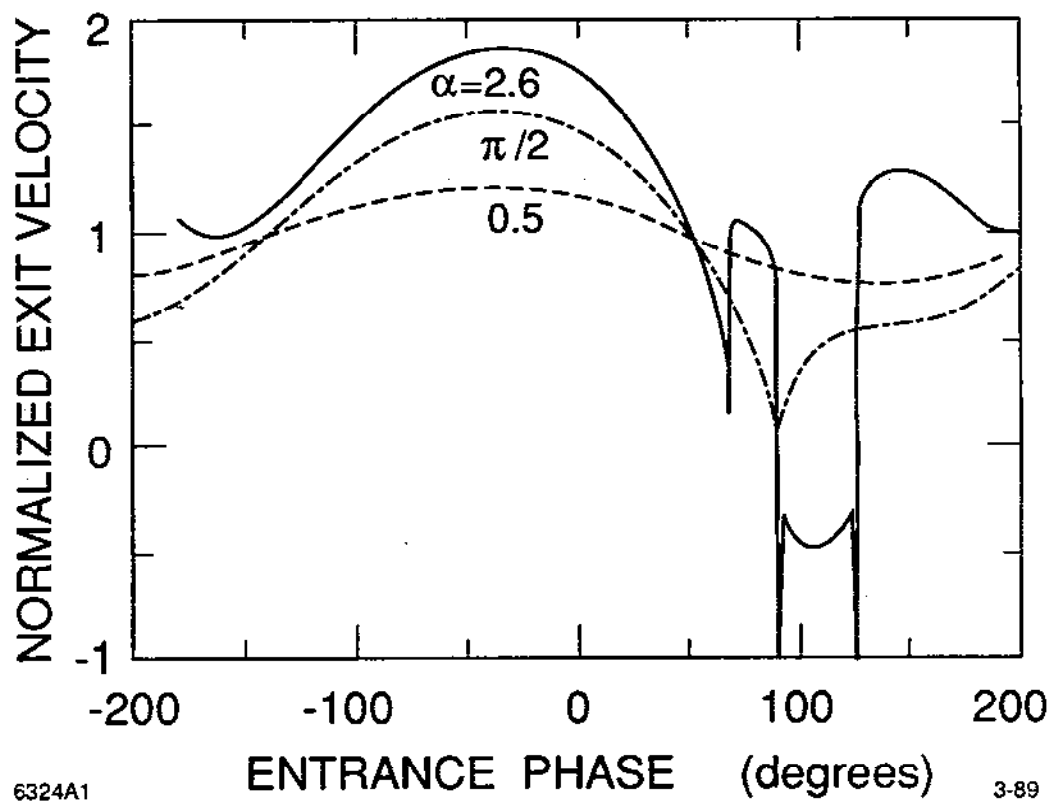


Fig. 2

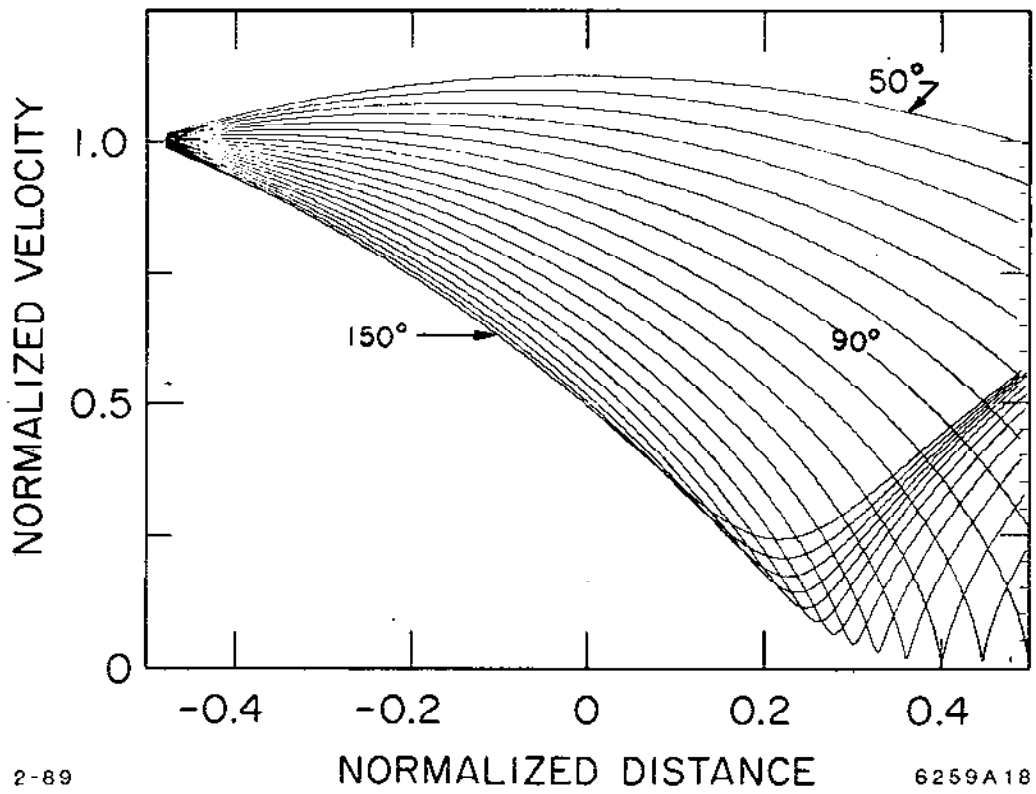
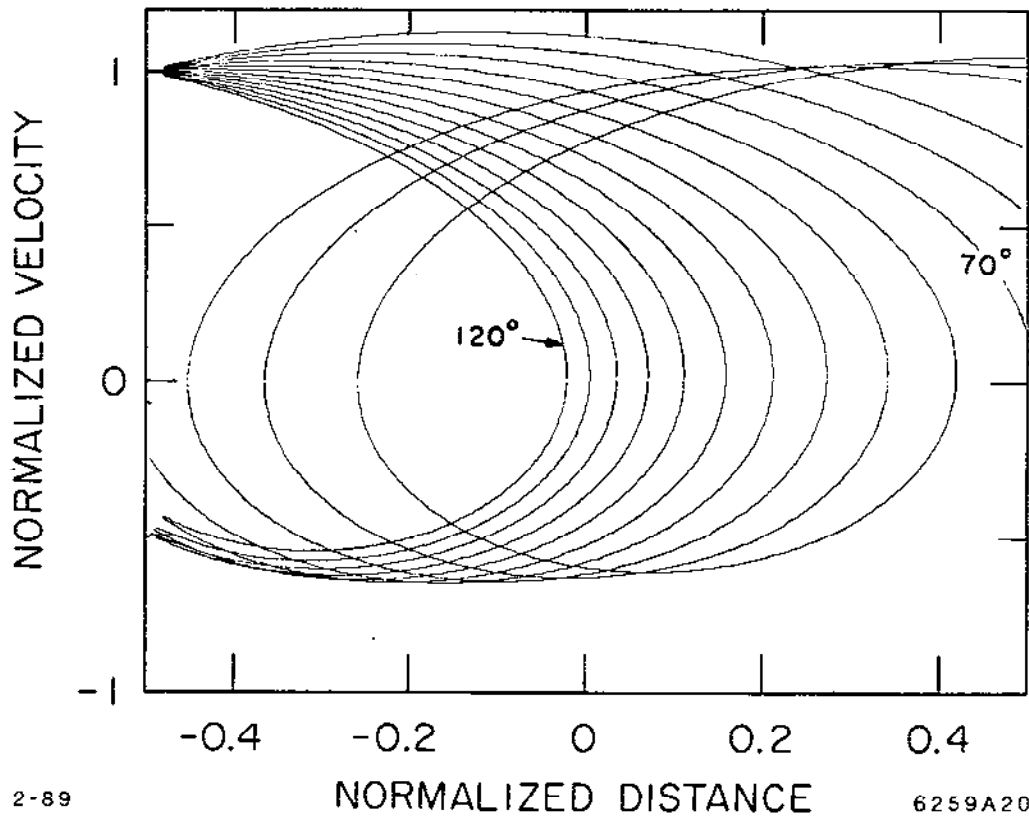


Fig. 3

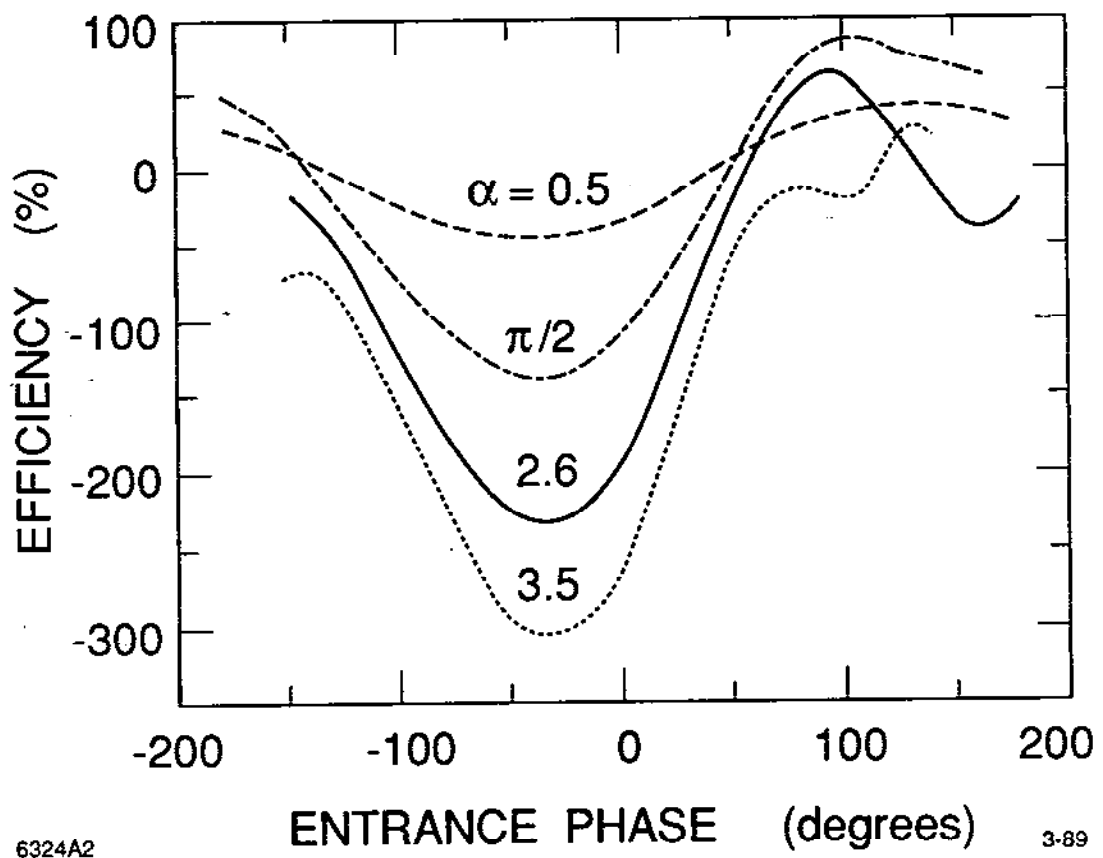


2-89

NORMALIZED DISTANCE

6259A20

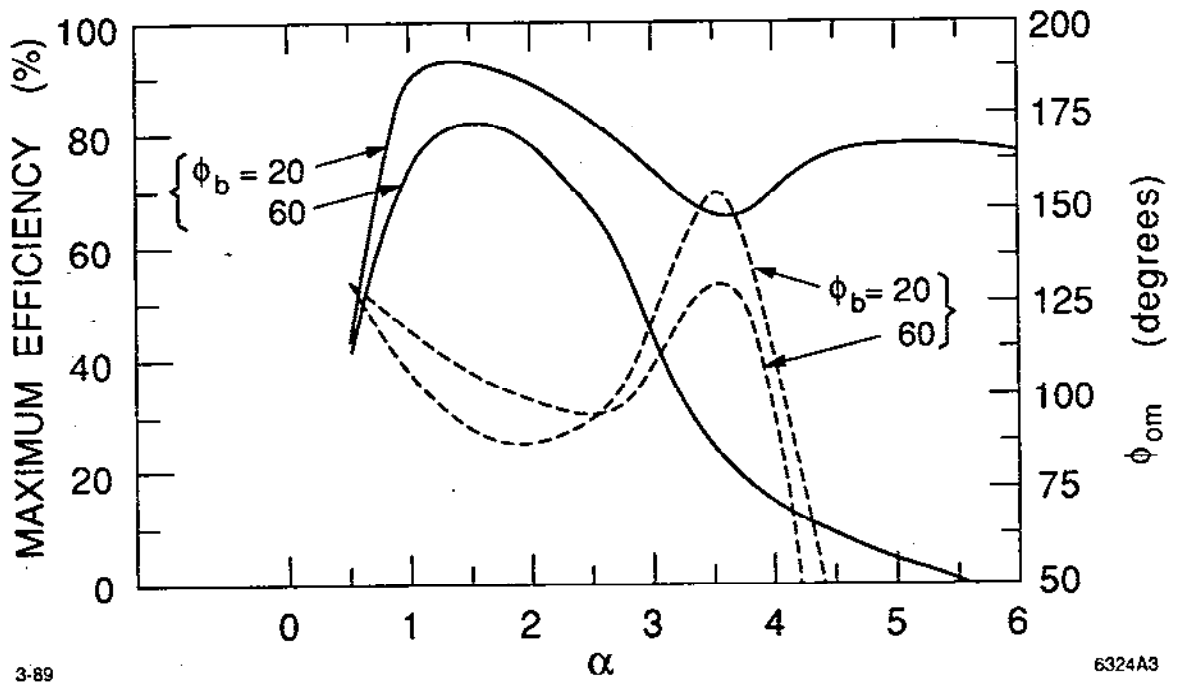
Fig. 4



6324A2

3-89

Fig. 5



3-89

6324A3

Fig. 6

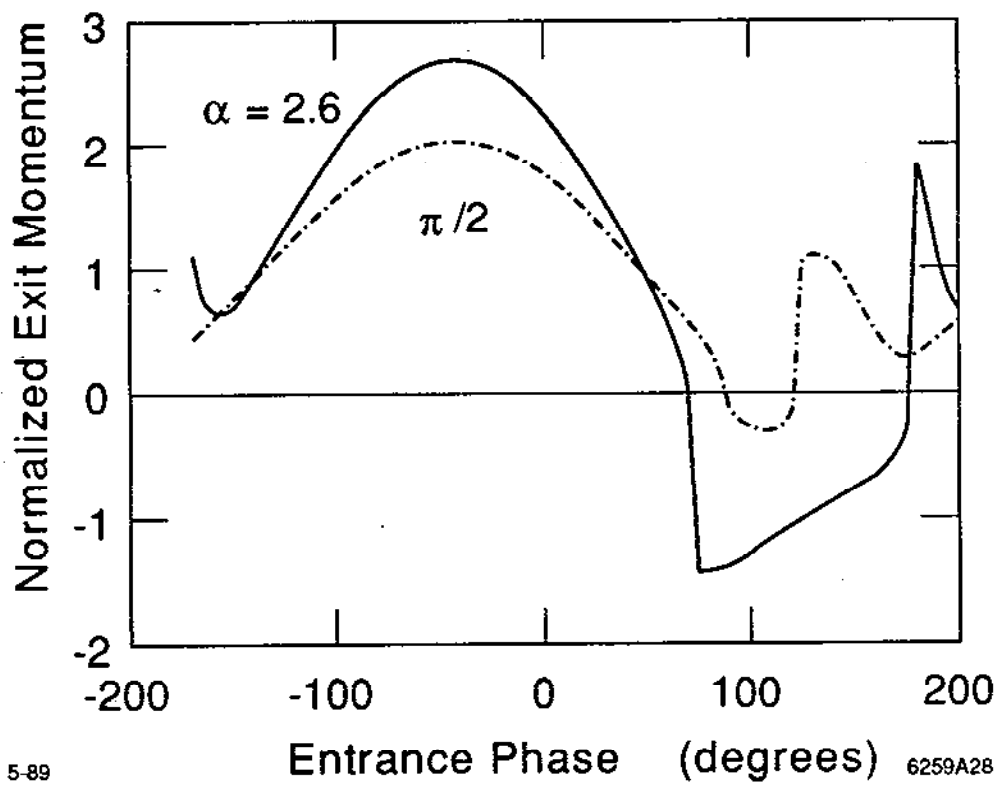
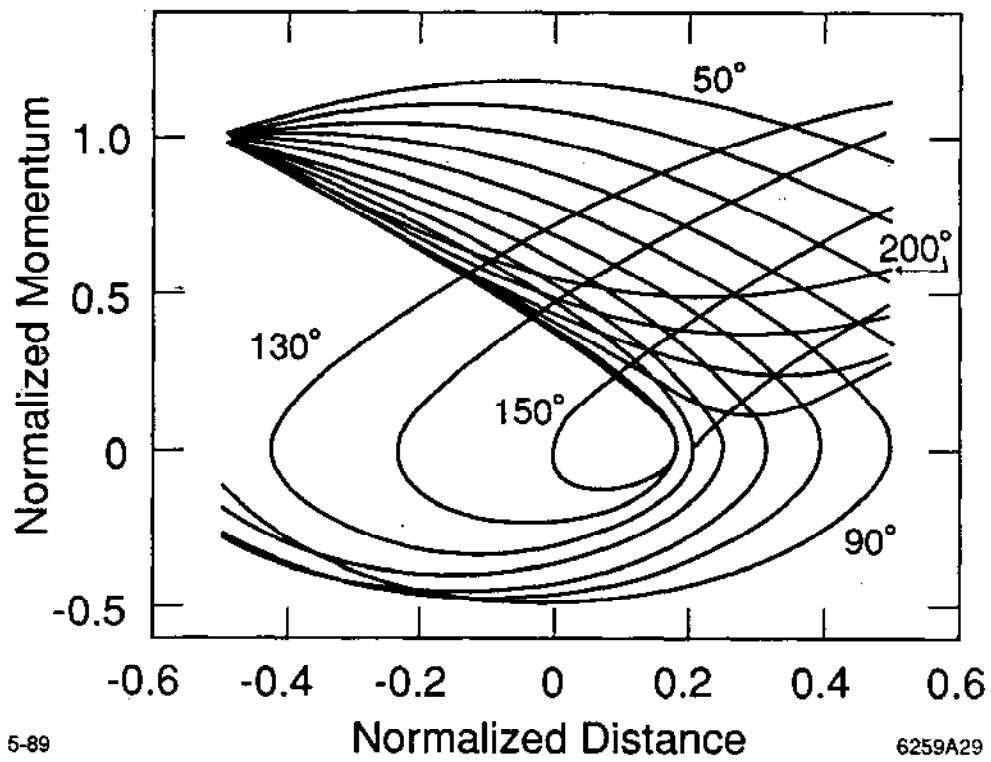


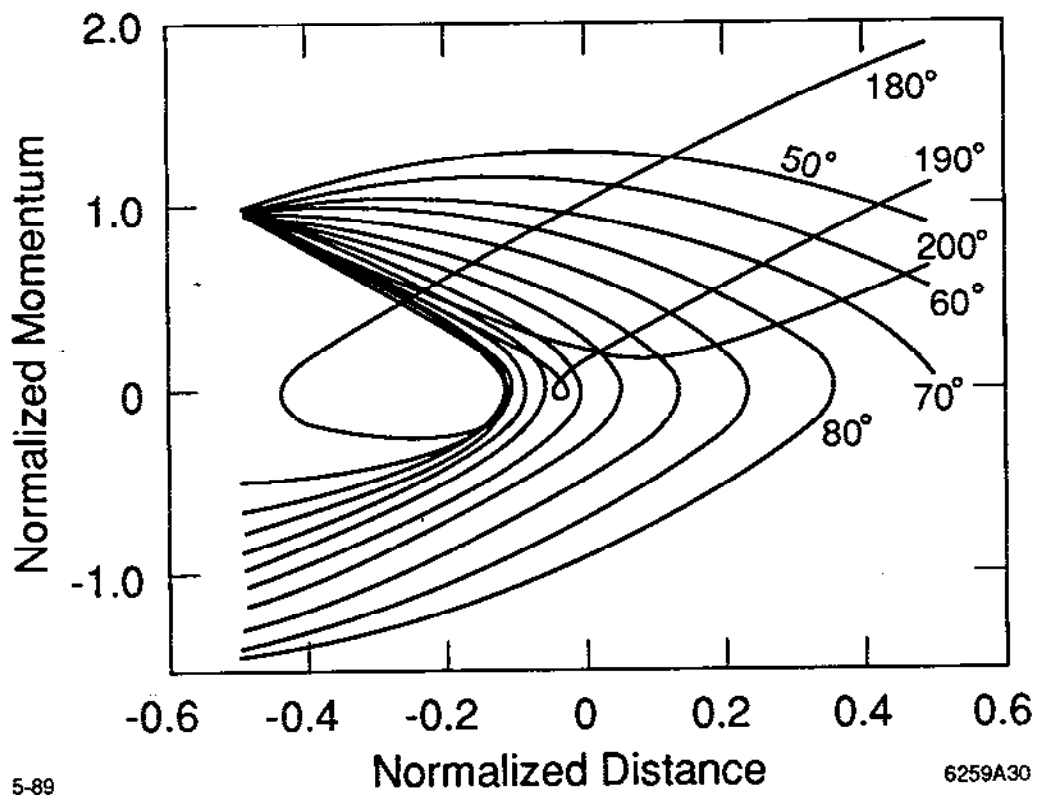
Fig. 7



5-89

6259A29

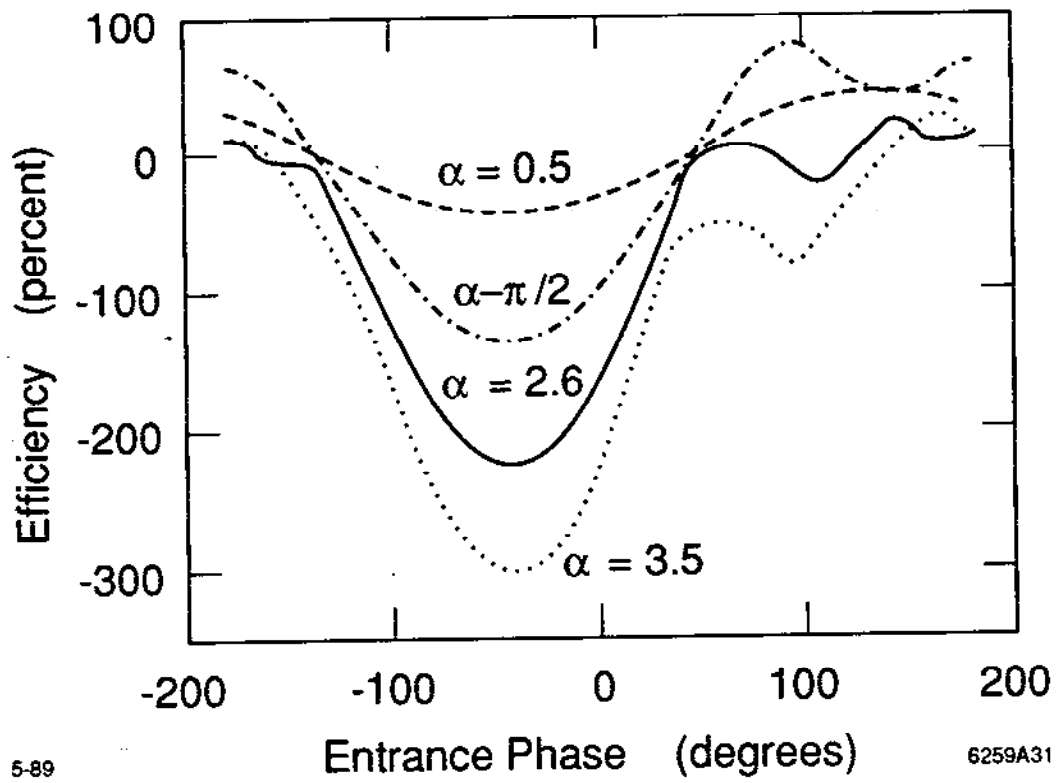
Fig. 8



5-89

6259A30

Fig. 9



5-89

6259A31

Fig. 10

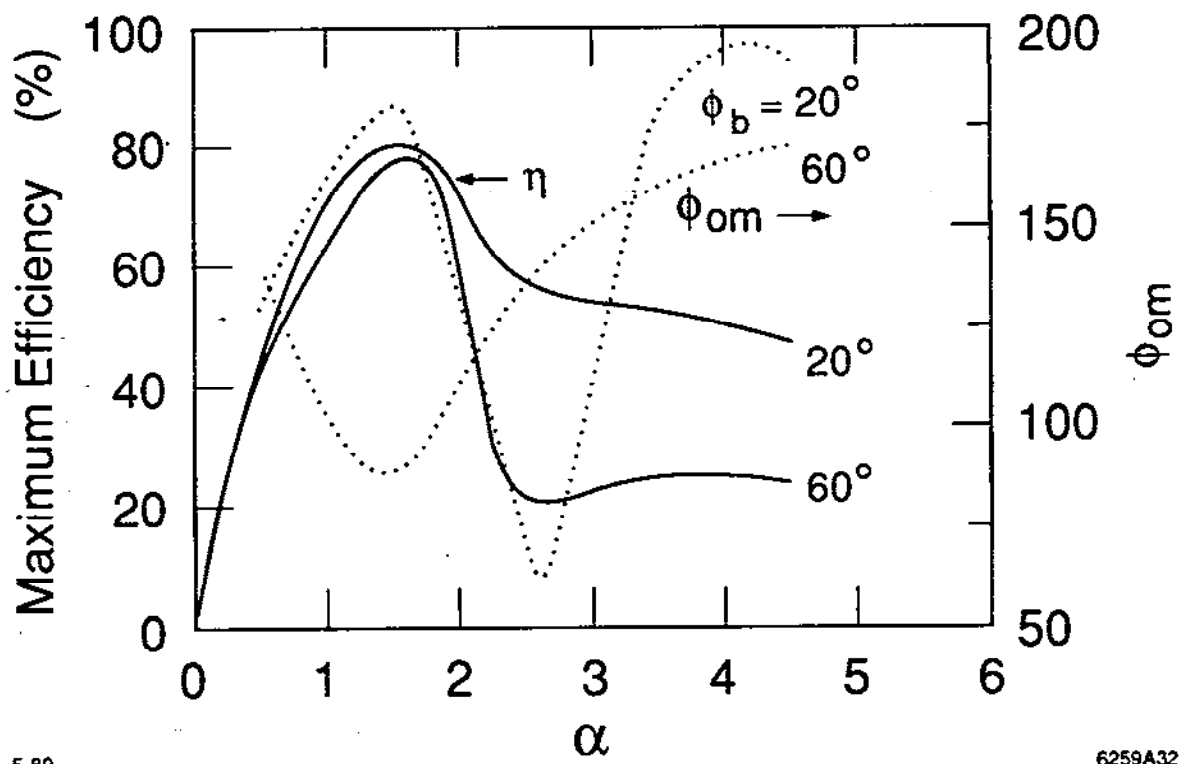


Fig. 11

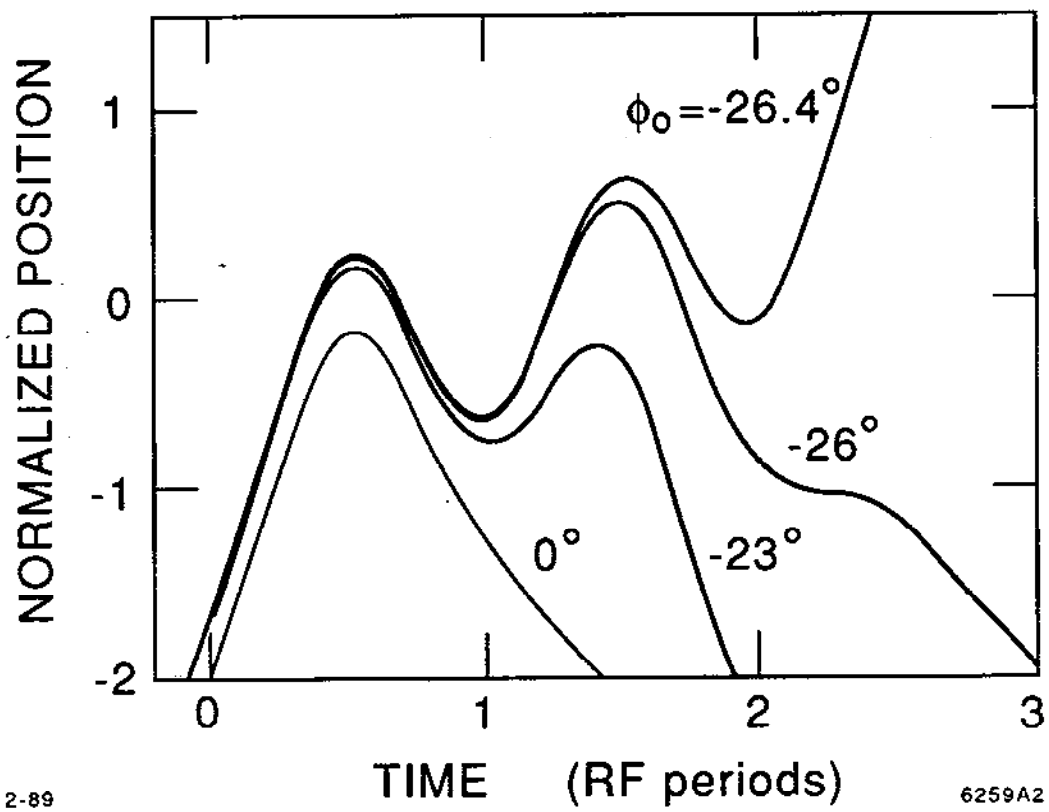


Fig. 12

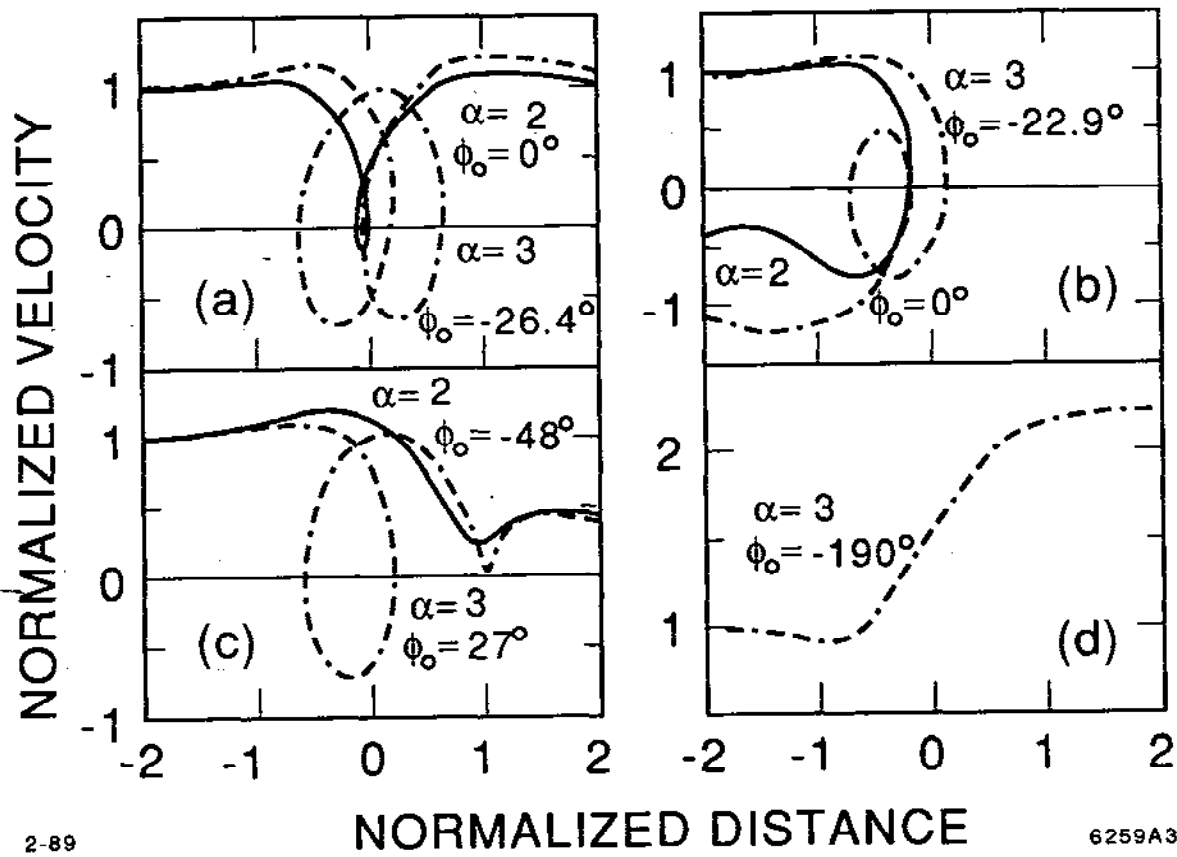


Fig. 13

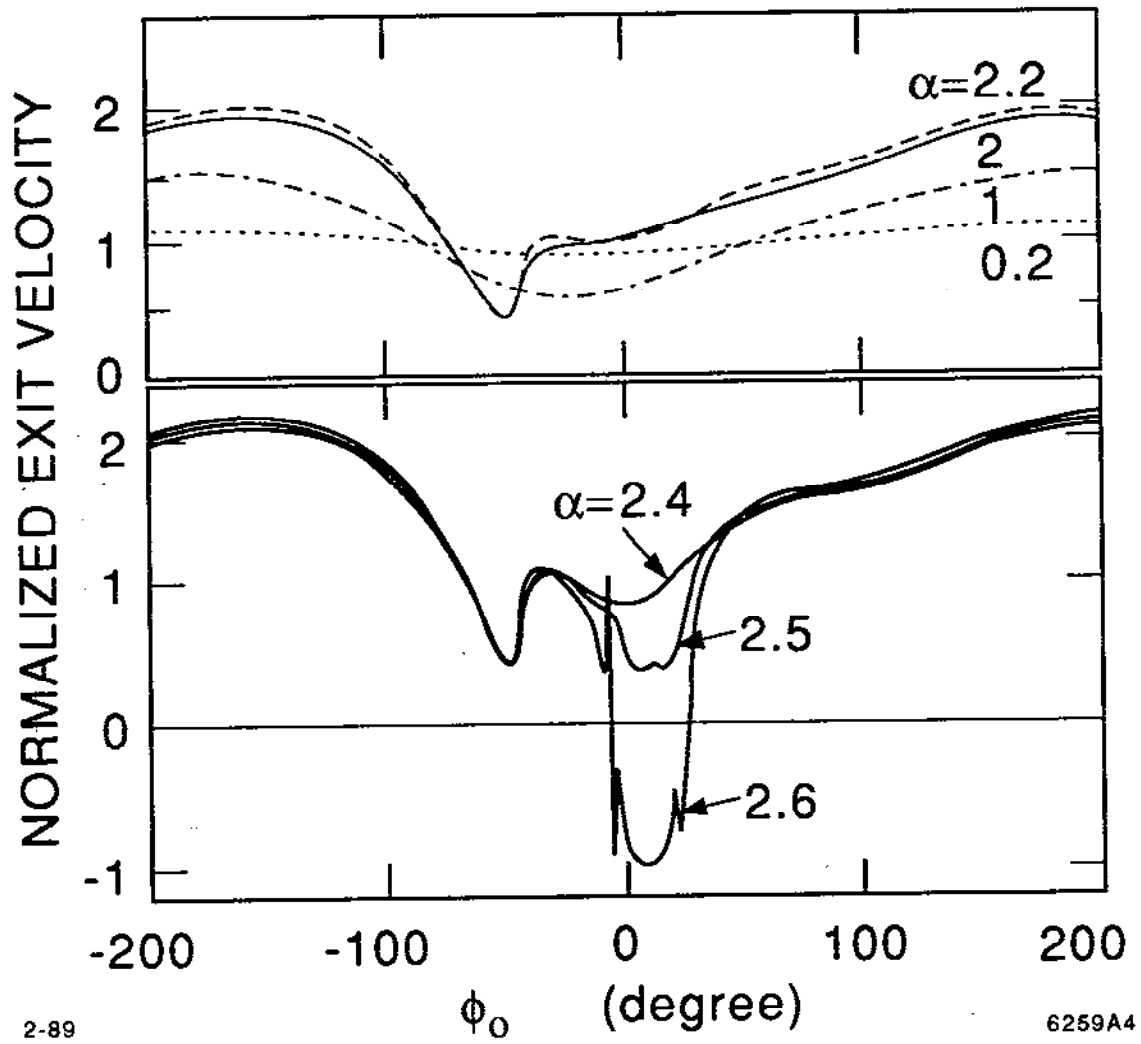
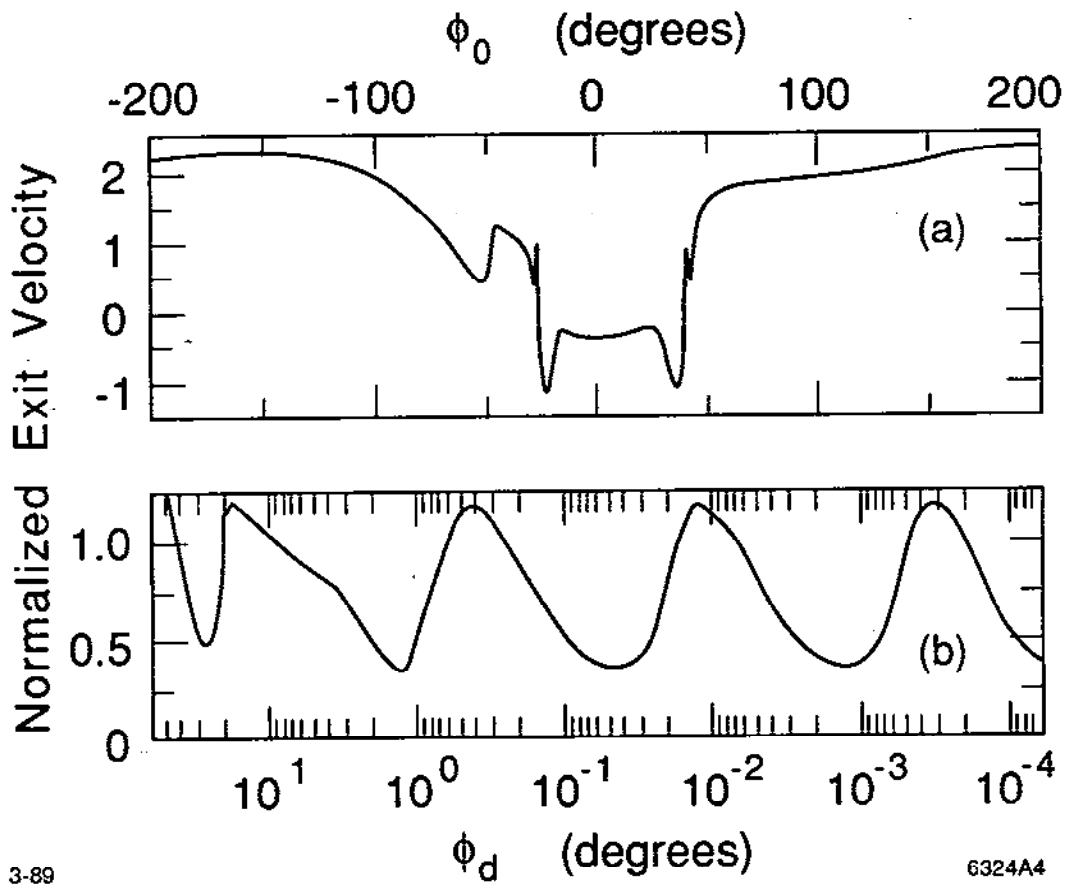


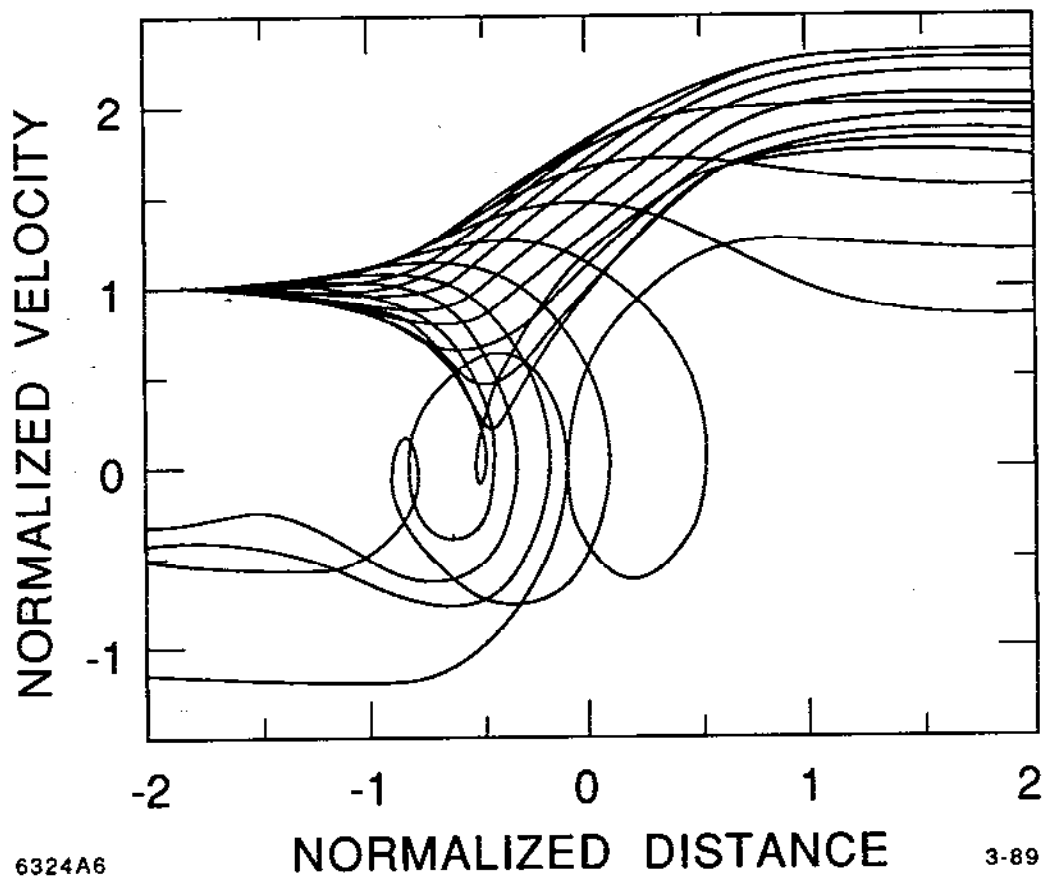
Fig. 14



3-89

6324A4

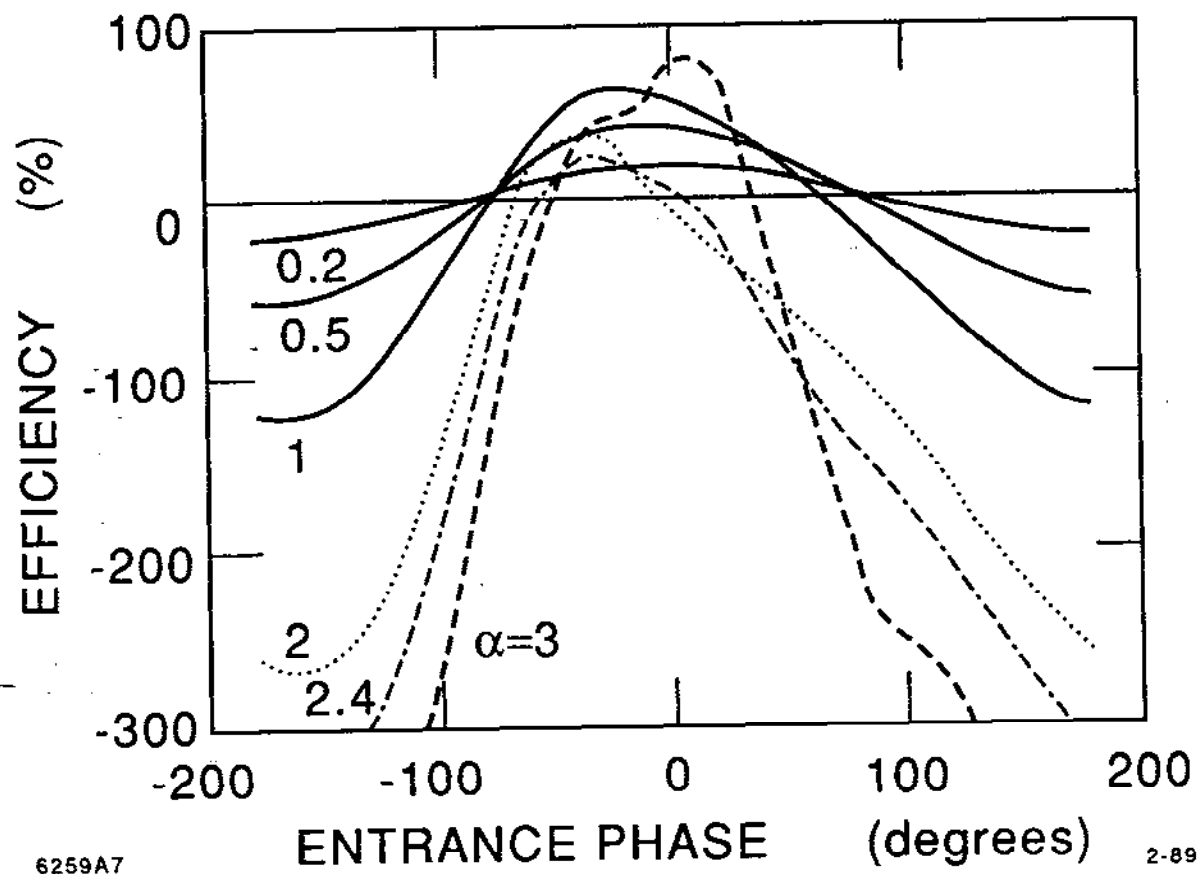
Fig. 15



6324A6

3-89

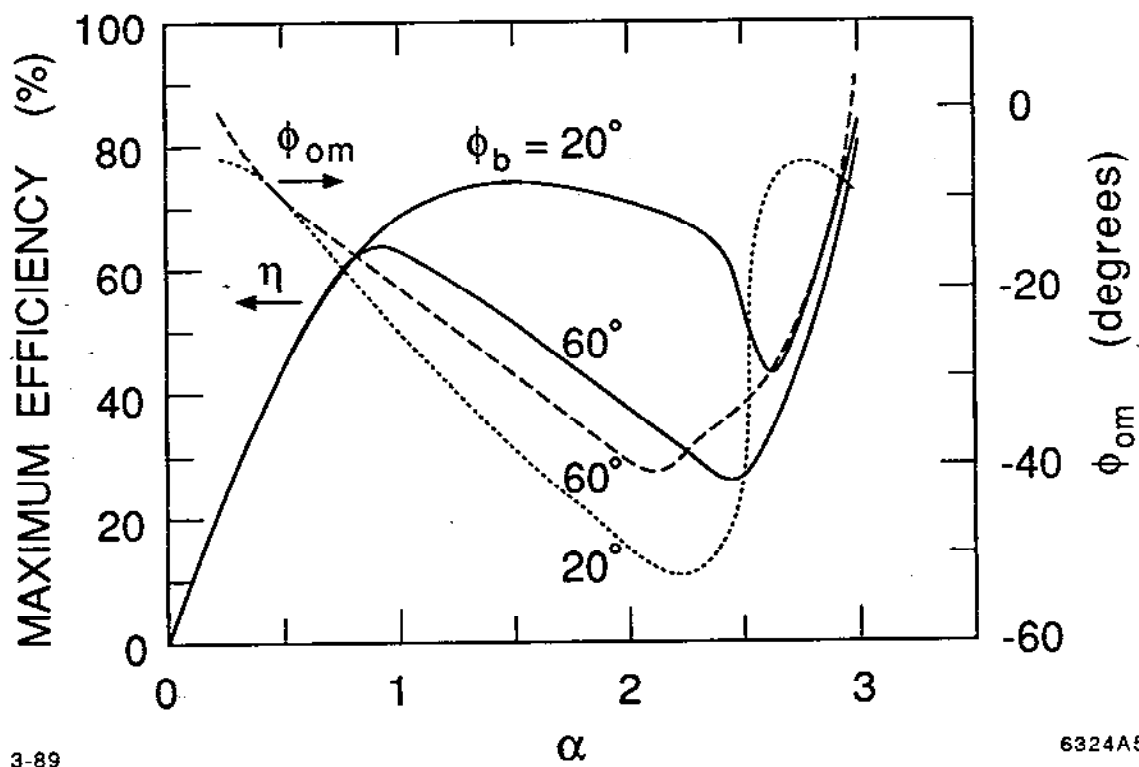
Fig. 16



6259A7

2-89

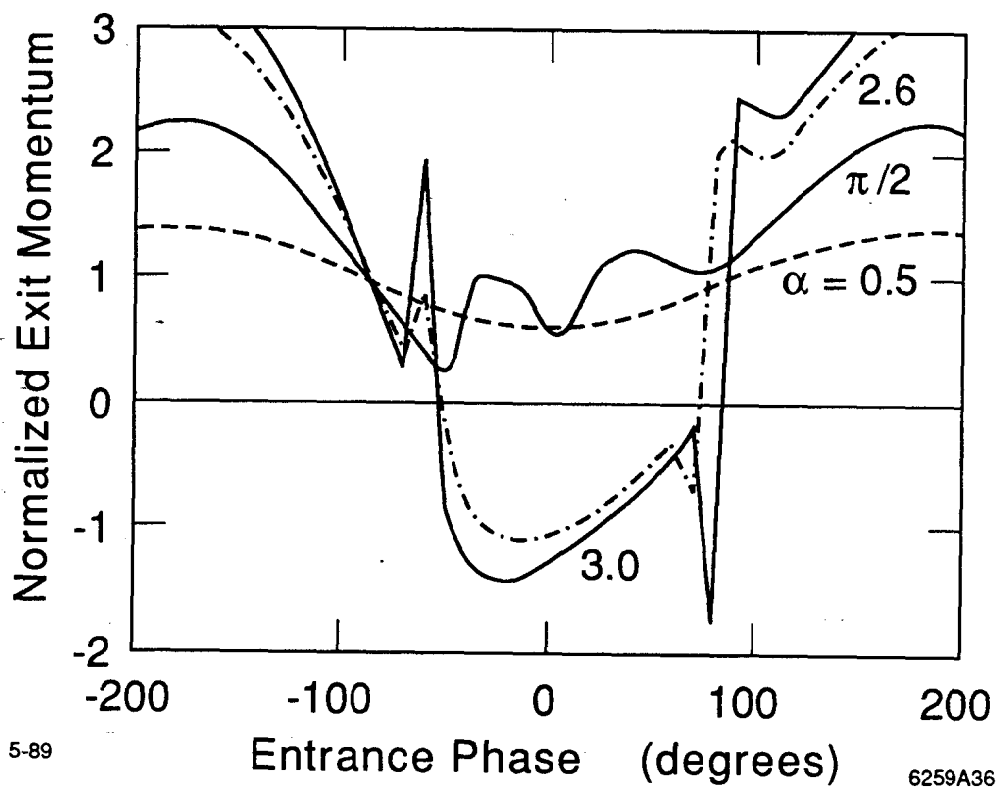
Fig. 17



3-89

6324A5

Fig. 18



5-89

6259A36

Fig. 19

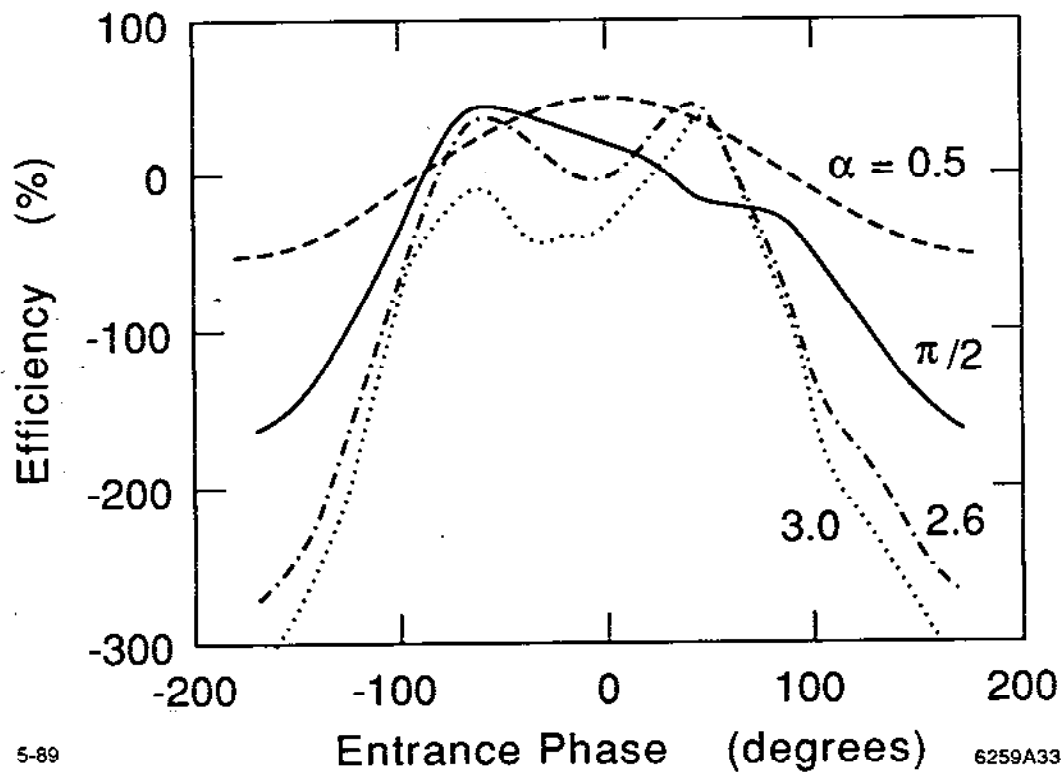


Fig. 20

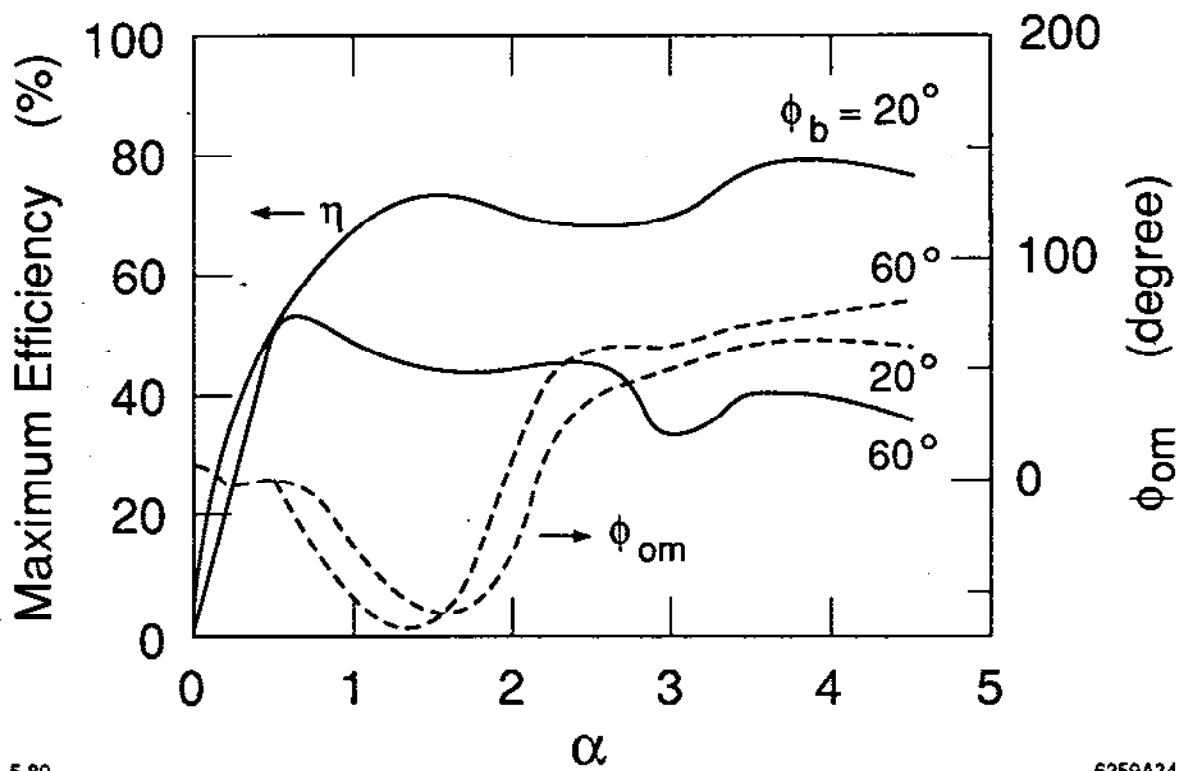
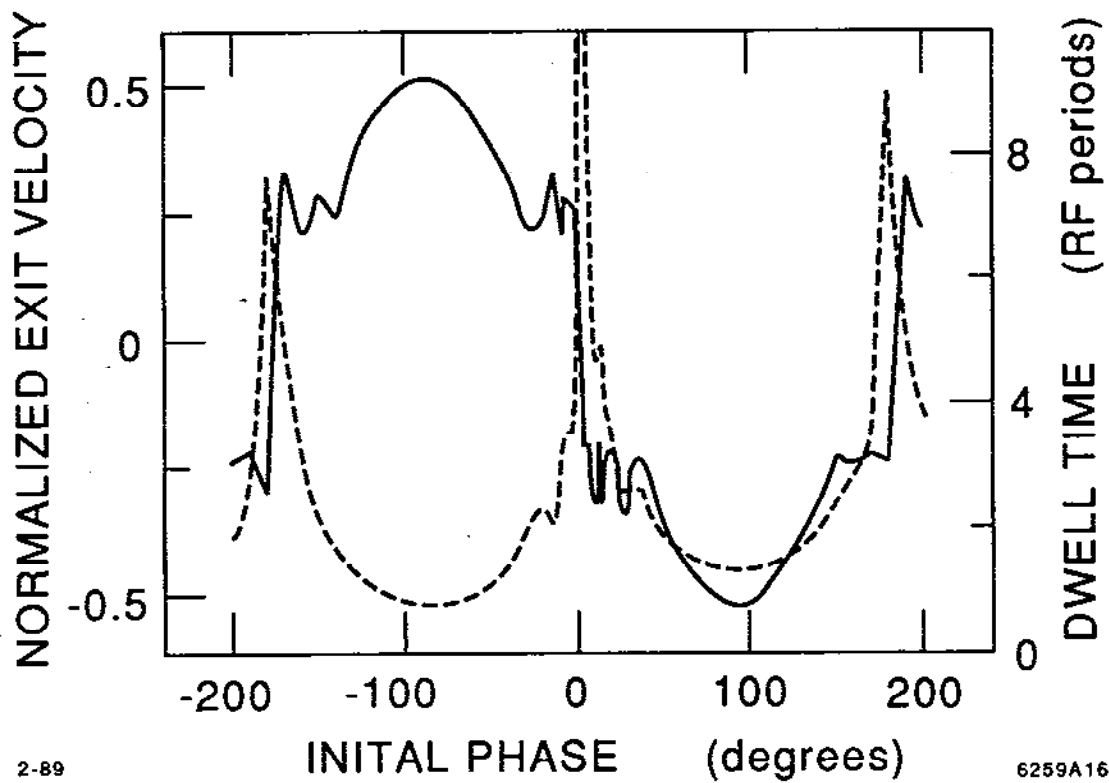


Fig. 21



2-89

6259A16

Fig. 22

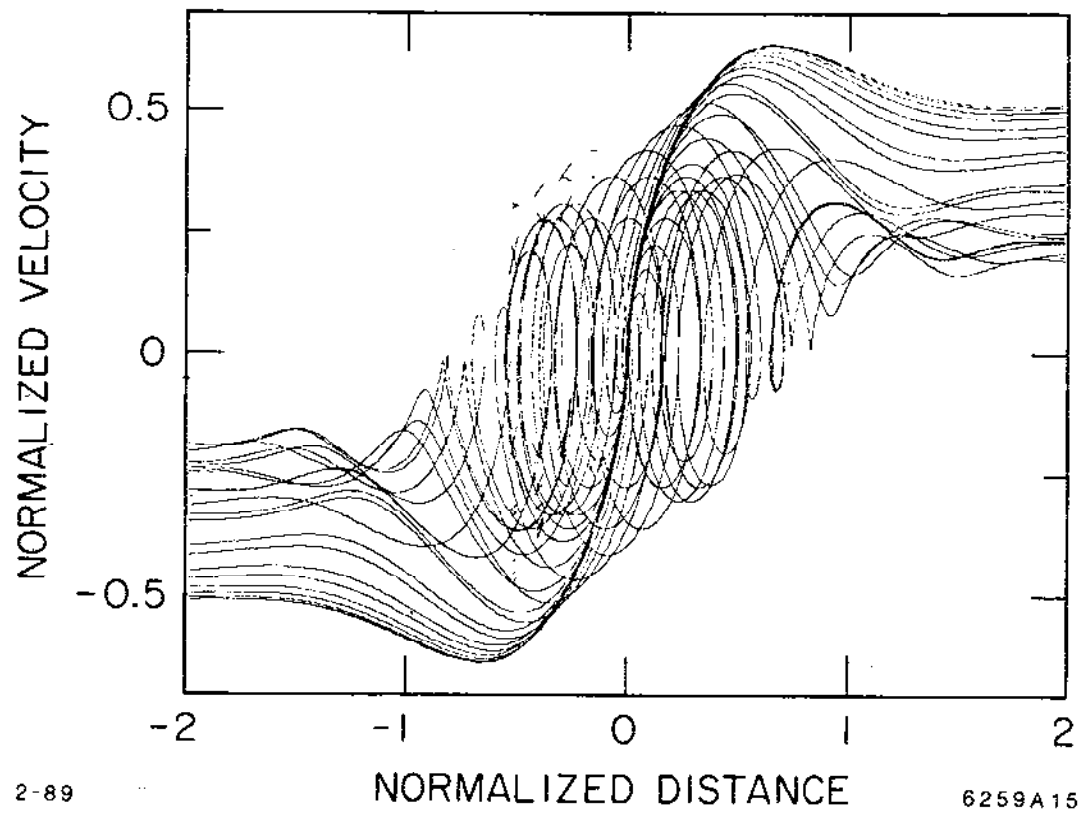


Fig. 23

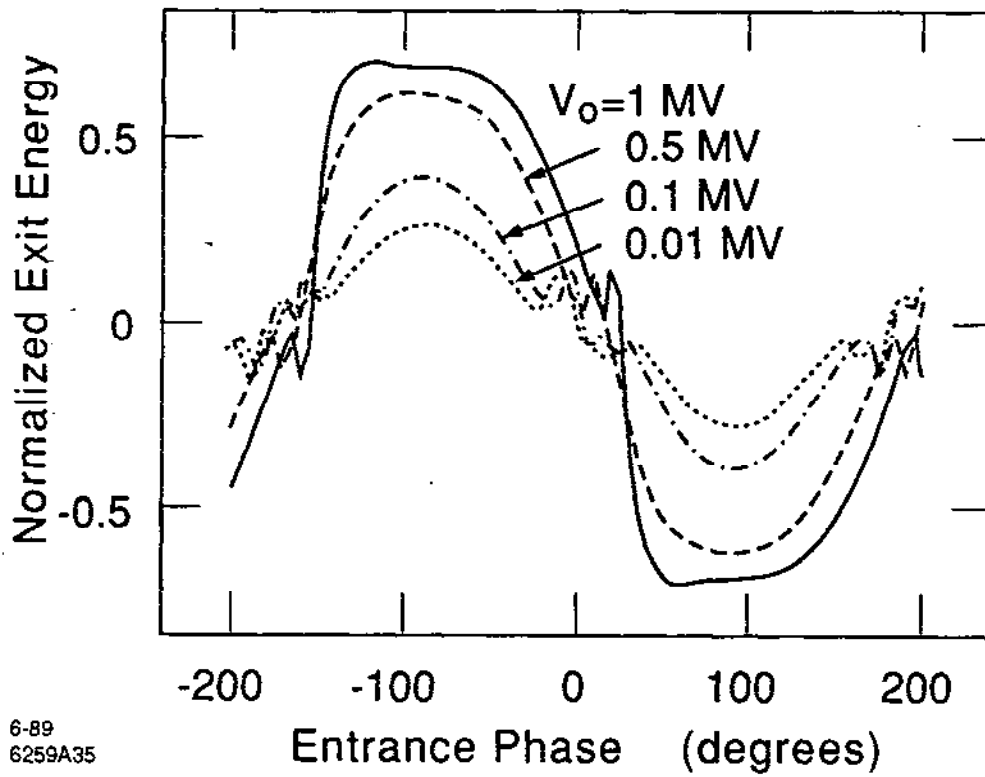
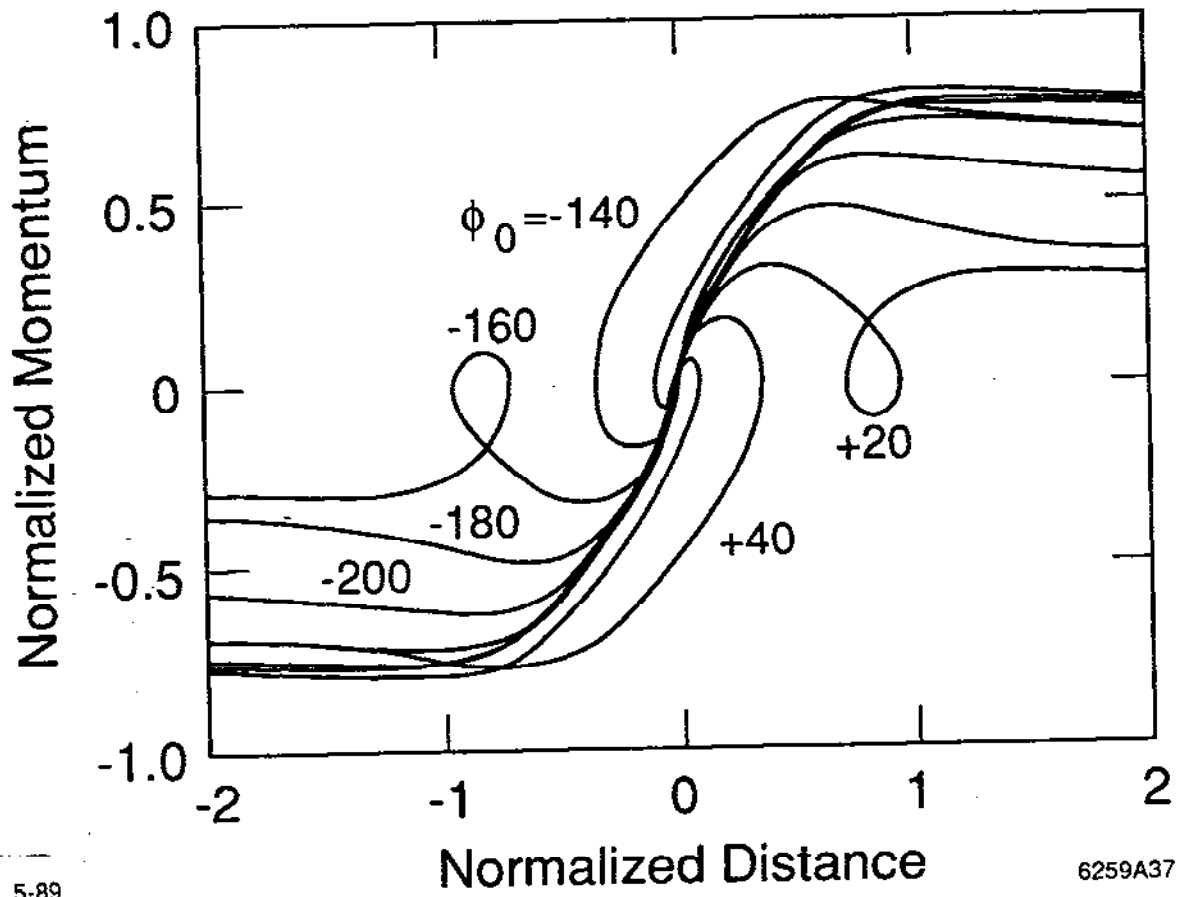


Fig. 24



5-89

6259A37

Fig. 25